

Ultralong-range polyatomic Rydberg molecules formed by a polar perturber

Seth T. Rittenhouse,¹ M. Mayle,^{2,*} P. Schmelcher,² and H. R. Sadeghpour¹

¹*ITAMP, Harvard-Smithsonian Center for Astrophysics, Cambridge, MA 02138*

²*Zentrum für Optische Quantentechnologien, Universität Hamburg,
Luruper Chaussee 149, D-22761 Hamburg, Germany.*

(Dated: September 23, 2018)

The internal electric field of a Rydberg atom electron can bind a polar molecule to form a giant ultralong-range stable polyatomic molecule. Such molecules not only share their properties with Rydberg atoms, they possess huge permanent electric dipole moments and in addition allow for coherent control of the polar molecule orientation. In this work, we include additional Rydberg manifolds which couple to the nearly degenerate set of Rydberg states employed in [S. T. Rittenhouse and H. R. Sadeghpour, *Phys. Rev. Lett.* **104**, 243002 (2010)]. The coupling of a set of $(n+3)s$ Rydberg states with the $n(l > 2)$ nearly degenerate Rydberg manifolds in alkali metal atoms leads to pronounced avoided crossings in the Born-Oppenheimer potentials. Ultimately, these avoided crossings enable the formation of the giant polyatomic Rydberg molecules with standard two-photon laser photoassociation techniques.

PACS numbers: 33.80.Rv, 31.50.Df

I. INTRODUCTION

The physics of Rydberg atoms and molecules has developed into a quasi-sustainable “ecosystem” over the last decade, mainly due to a) the exaggerated properties of Rydberg atoms and molecules (long lifetimes, large sizes, and scalability), and b) exquisite experimental control over these properties through the advent of ultracold atomic Rydberg samples [1, 2]. Some landmark developments over the last few years in the field of Rydberg physics have been the creation of a frozen Rydberg gas [3], the demonstration of a Rydberg blockade scheme and the subsequent realization of a Rydberg qubit gate [4–7], the formation of ultralong-range isotropic Rydberg molecule [8], the creation ultracold neutral plasmas [9], as well as the formation of highly-magnetized Rydberg antihydrogen atoms [10]. These rapid advances now allow for few-body and many-body effects to be realized in laboratory settings and be prototyped for simulation of strongly interacting spin chains [11–13]. The other ingredient of our proposed polyatomic Rydberg complex, namely, ultracold polar molecules, have also been touted as toy models for the simulation of many-body condensed systems and for the realization of quantum gates [14]. A main appeal of polar molecules is that they may possess sizeable permanent dipole moments.

In this work, we harness the long-range interaction of a Rydberg atom with a polar molecule (Rb is used as an ubiquitous example, but other alkali metal atoms would serve the purpose), to demonstrate that ultralong-range polyatomic molecules with enormous permanent dipole moments can form from combining a Rydberg atom and

a polar molecule. This system was first studied in [15] where it was shown that the Rydberg electron can be used to “drag” the polar molecule into a preferred orientation and that this process can be controlled by a Raman microwave pulse scheme. Ultralong range Rydberg molecules in general came in vogue after a proposal that such molecules could form from zero-range interaction of electrons with ground state atoms [16]. The recent experimental realization of a class of such molecules [8] has led to revived theoretical and experimental activity [17, 18].

The interaction of the polar perturber with the Rydberg atom strongly couples the field-free atomic Rydberg states by means of the dipole’s electric field. In [15], the mixing of states was restricted to the nearly degenerate (negligible quantum defects) manifold of Rydberg states in $\text{Rb}(nl \gtrsim 3)$. In the present work, we extend our previous study by going beyond this degenerate perturbation theory approach. In this manner, the effect of additional Rydberg orbitals on the molecular Born-Oppenheimer (BO) potentials is probed. In particular, the proximity of the $n(l > 2)$ Rydberg manifold to a single $(n+3)s$ state introduces a strong coupling, allowing for the experimental preparation of the proposed polyatomic Rydberg molecules via a standard two-photon laser excitation.

The paper is outlined as follows. In section II the model Hamiltonian describing the polar molecule perturber is introduced. The adiabatic Hamiltonian for the full Rydberg atom plus polar molecule complex is subsequently provided in section III. The resulting adiabatic potential surfaces are discussed in section IV. In section V we discuss the admixture of s -wave electron character in the giant Rydberg molecule. We conclude by a brief summary and an outlook on further research directions in section VI.

*Present address: JILA, University of Colorado and National Institute of Standards and Technology, Boulder, Colorado 80309-0440, USA.

II. POLAR MOLECULE MODEL HAMILTONIAN

Before we discuss the properties of the proposed polyatomic Rydberg molecules, we must introduce an effective Hamiltonian for the molecular perturber. In this context, we model the polar molecule as a two-level molecule in which the opposite parity states are mixed in the presence of an external field, i.e.,

$$H_{mol} = \begin{pmatrix} 0 & d_0 F_{ext} \\ d_0 F_{ext} & \Delta \end{pmatrix}, \quad (1)$$

where Δ is the zero field splitting between the two molecular states (as in a Λ -doublet molecule), d_0 is the permanent dipole moment of the molecule in the body fixed frame, and F_{ext} is an electric field external to the polar molecule. Specifically, the external field stems from the Rydberg electron and the Rydberg core, i.e.,

$$F_{ext}(\vec{R}, \vec{r}) = e \left[\frac{\hat{R}}{R^2} + \frac{(\vec{r} - \vec{R})}{|\vec{r} - \vec{R}|^3} \right], \quad (2)$$

where e is the electron charge, \vec{R} is the core-polar molecule separation vector and \vec{r} is the position of the Rydberg electron with respect to the core. In other words, (1) describes the coupling between the internal state of the polar molecule and the Rydberg atom.

It should be noted that (1) only depends on the magnitude of the external field, which is appropriate for static, homogeneous fields. For a rigid rotor molecule, such as KRb, the rotation of the molecule happens on much slower time scales than the Rydberg electron orbital time. In this case, the coupling between the Rydberg atom and the polar molecule accounts for the rotation of the molecule,

$$V_{mol}(\vec{R}) = -\vec{d} \cdot \vec{F}_{ext}, \quad (3)$$

where \vec{d} is the rigid rotor dipole moment. This interaction leads to BO potential surfaces which depend on both \vec{R} and the orientation of \vec{d} with respect to \vec{R} ; this more complete treatment is the subject of an ongoing study. In contrast, a Λ doublet molecule, such as OH, has a permanent dipole moment that arises from the interaction of two opposite parity electronic (e, f) states. Rotational transition energies in Λ -doublet molecules are usually orders of magnitude larger than the typical doublet splitting energies. For the fields provided by highly excited Rydberg atoms, of order $F_{ext} \sim 10^{-6}$ a.u., our model Hamiltonian (1) thus provides an excellent description of such molecules.

The electron-dipole interaction in (3) and in the off-diagonal elements of (1) has a critical value. If the dipole moment, d_0 , is larger than the Fermi-Teller critical value, $d_c = 1.63$ D, an infinite number of bound states form [19]. Furthermore, an electron scattering off a super critical

dipole ($d_0 > d_c$) is sensitive to the detailed, short-range structure of the polar molecule. To avoid the complication of super-critical dipole scattering and electron transfer from the Rydberg atom to the polar molecule, we will deal exclusively with polar molecules whose dipole moments are subcritical, i.e., $d_0 < 1.63$ D.

III. THE ADIABATIC HAMILTONIAN

For simplicity, we assume that the external electric field is along the intermolecular axis, such that (2) becomes

$$F_{ext}(\vec{R}, \vec{r}) = \frac{e}{R^2} + \frac{e \cos \theta_{\vec{r}-\vec{R}}}{|\vec{r} - \vec{R}|^2} \quad (4)$$

where $\theta_{\vec{r}-\vec{R}} = (\vec{r} - \vec{R}) \cdot \vec{R} / R |\vec{r} - \vec{R}|$. This means that the projection m of the Rydberg electron angular momentum along \vec{R} is conserved. To find the BO potentials, we solve the adiabatic Schrödinger equation at fixed polar molecule location $\vec{R} = R\hat{z}$,

$$H_{ad}\psi(R; \vec{r}, \sigma) = U(R)\psi(R; \vec{r}, \sigma), \quad (5)$$

with

$$H_{ad} = H_A + H_{mol}. \quad (6)$$

The first term, $H_A = -\frac{\hbar^2}{2m_e}\nabla_r^2 + V_l(r)$, describes the unperturbed Rydberg atom; the core penetration, scattering, and polarization effects of its valence electron are accounted for by the l -dependent model potential $V_l(r)$ [20], giving rise to the quantum defects of the low angular momentum Rydberg states. m_e is the electron mass, ψ is the electron wave function, and σ is a coordinate signifying the internal states of the polar molecule. The eigenvalues $U(R)$ serve as the sought-after BO potentials for the polar perturber. To solve (5), the total wave function is expanded in the basis $\{\psi_{nlm}(\vec{r})|\pm\rangle\}$ where $\psi_{nlm}(\vec{r})$ is an unperturbed Rydberg orbital and $|\pm\rangle$ are the polar molecule parity states. The atomic and molecular degrees of freedom are coupled by the electric field (4) that mixes both the Rydberg orbitals as well as the parity states of the polar molecule, cf. (1).

In [15], the BO potentials were found using degenerate perturbation theory in the (nearly) degenerate set of Rydberg orbitals $\{\psi_{n(l>2)0}(\vec{r})\}$. The molecular Hamiltonian (1) can be prediagonalized to yield the eigenvalues

$$\varepsilon(F_{ext}) = d_0 \left(F_c \pm \sqrt{F_{ext}^2 + F_c^2} \right), \quad (7)$$

where $F_c = \Delta/2d_0$ is the critical external field strength at which the molecule becomes completely polarized. Inserting in (7) for F_{ext} the R -dependent eigenstates of the Rydberg atom exposed to the field (4) results in the potentials found in [15]. A more complete treatment of the

system requires that the total adiabatic Hamiltonian is diagonalized in a complete set of Rydberg orbitals. Because in the latter case, the orbitals are in general not degenerate, the prediagonalization scheme cannot be directly used beyond the degenerate perturbation theory.

In the present work, we go beyond the degenerate perturbation theory framework adapted in [15]. To this end, the Hamiltonian (6) is diagonalized in an extended basis set comprising several Rydberg n manifolds. By construction, the atomic Hamiltonian H_A is diagonal in the Rydberg basis $\{\psi_{n'l_0}(r)\}$,

$$\left\langle \psi_{n'l'0}, \sigma' \left| -\frac{1}{2} \nabla_r^2 + V_l(r) \right| \psi_{n'l_0}, \sigma \right\rangle = \Delta \delta_{\sigma, -\delta_{n'l'n} \delta_{l'l} \delta_{\sigma'\sigma}} - \delta_{n'l'n} \delta_{l'l} \delta_{\sigma'\sigma} \frac{1}{2(n-\mu_l)^2} \frac{\cos \theta_{\vec{r}-\vec{R}}}{|\vec{r}-\vec{R}|^2} = \begin{cases} -\sqrt{4\pi} \sum_l \frac{R^{l-1}}{r^{l+1}} \frac{l\sqrt{2l+1}}{(2l+1)} Y_{l0}(\theta, \phi), & r > R \\ \sqrt{4\pi} \sum_l \frac{r^l}{R^{l+2}} \frac{(l+1)\sqrt{2l+1}}{(2l+1)} Y_{l0}(\theta, \phi), & r < R \end{cases}$$

where μ_l is the quantum defect for the l -th partial wave Rydberg state and σ denotes the parity state of the polar molecule. The quantum defects used in this work are those for the rubidium atom [2]: $\mu_s = 3.13$, $\mu_p = 2.65$, $\mu_d = 1.35$, $\mu_f = 0.016$, and $\mu_{l>3} \approx 0$. While our focus is on Rb, the method can be extended to any highly excited Rydberg atom by using the appropriate quantum defects.

The off-diagonal matrix elements of (6) are due to H_{mol} which couples the Rydberg electron states to the internal parity states of the polar molecule. They are determined by evaluating the integrals

$$\langle \psi_{n'l'0} | F_{ext} | \psi_{n'l_0} \rangle = -e \int d^3r \psi_{n'l'0}^*(\vec{r}) \frac{\cos \theta_{\vec{r}-\vec{R}}}{|\vec{r}-\vec{R}|^2} \psi_{n'l_0}(\vec{r}). \quad (8)$$

An intuitive closed form of (8) is obtained if we expand the electron electric field contribution in spherical harmonics. Using the multipole expansion of [21] yields

$$\frac{\cos \theta_{\vec{r}-\vec{R}}}{|\vec{r}-\vec{R}|^2} = \begin{cases} -\sqrt{4\pi} \sum_l \frac{R^{l-1}}{r^{l+1}} \frac{l\sqrt{2l+1}}{(2l+1)} Y_{l0}(\theta, \phi), & r > R \\ \sqrt{4\pi} \sum_l \frac{r^l}{R^{l+2}} \frac{(l+1)\sqrt{2l+1}}{(2l+1)} Y_{l0}(\theta, \phi), & r < R \end{cases} \quad (9)$$

We note that, with some generalization, this procedure can also be used to evaluate the interaction matrix elements between a permanent dipole and the Rydberg electron, cf. (3). Using (9), the off diagonal matrix elements of (5) are given by

$$\left\langle \psi_{n'l'0} \left| \frac{\cos \theta_{\vec{r}-\vec{R}}}{|\vec{r}-\vec{R}|^2} \right| \psi_{n'l_0} \right\rangle = \sqrt{(2l'+1)(2l+1)} \sum_{l''=|l-l'|}^{l+l'} \begin{pmatrix} l & l' & l'' \\ 0 & 0 & 0 \end{pmatrix}^2 \times \left[(l''+1) \frac{1}{R^{l''+2}} \int_0^R r^{l''+2} R_{nl}^*(r) R_{n'l'}(r) dr - R^{l''-1} l'' \int_R^\infty \frac{1}{r^{l''-1}} R_{nl}^*(r) R_{n'l'}(r) dr \right], \quad (10)$$

where $R_{nl}(r)$ is the radial wave function for an electron in the nl Rydberg state.

The adiabatic Hamiltonian matrix assumes the following form,

$$\bar{H}_{ad} = \begin{pmatrix} \bar{E}_{Ryd} & d_0 \bar{F} \\ d_0 \bar{F} & \Delta \bar{I} + \bar{E}_{Ryd} \end{pmatrix}, \quad (11)$$

where \bar{I} is the unity matrix, \bar{E}_{Ryd} is the diagonal matrix representation of H_A , and \bar{F} is the electric field matrix whose elements are given by (10) with a diagonal offset of $1/R^2$ due to the contribution of the electric field from the positive ionic core to the total electric field, as defined in (4). The BO potentials are found by diagonalizing the matrix (11) at each R . Special attention must thereby be drawn to the actual size of the basis set in order to ensure convergence of the potentials.

IV. BORN-OPPENHEIMER POTENTIALS

In [15], it was assumed that for $l > 2$, the Rydberg orbitals of Rb are degenerate and that only this degenerate set of states is required to converge the BO potentials. Here we extend this treatment to including additional Rydberg orbitals and the small, but finite, f -wave quantum defect. Figure 1 compares the BO potentials using degenerate perturbation theory (solid curves, as in [15]) to those found by including the f -wave quantum defect (dotted curves) for the $n = 25$ state of rubidium; a polar molecule dipole moment of $d_0 = 0.40$ a.u., and a zero-field splitting of $\Delta = 1.85 \times 10^{-7}$ a.u. is considered.

We reiterate some of the most salient features of the proposed molecules. The modulations that form a series of wells reflect the oscillatory nature of the Rydberg electron wave function. The outer most wells in the lowest two potentials are deep enough to support many vibrational levels. The resulting giant polyatomic Rydberg molecules share several features with previ-

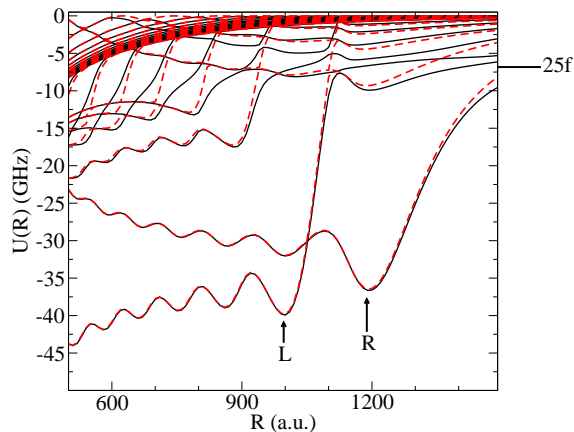


FIG. 1: The BO potentials for the Rb($n = 25$) Rydberg atom and a polar molecule are shown. The potentials are calculated at the level of degenerate perturbation theory including (dashed red curves) and ignoring (solid black curves) the f -wave quantum defect of the Rydberg electron. The polar perturber in this example is a molecule with a dipole moment $d_0 = 0.40$ a.u. and a zero field splitting $\Delta = 1.85 \times 10^{-7}$ a.u.

ously predicted homonuclear Rydberg molecules, the so called “trilobite” molecules [16, 22, 23]. The size of these molecules scales as $R_{ryd} \propto n^2$ and the well depths scale as $V_D \propto d_0/n^3$. Unlike for homonuclear Rydberg molecules, the anisotropic nature of the electron-dipole interaction creates two different internal configurations. Corresponding to the well labelled R in figure 1, in one configuration the dipole of the polar molecule is oriented towards the positive core. In the other configuration – labelled L – the dipole of the polar molecule is oriented away from the positive core.

As anticipated, inclusion of the small f -wave quantum defect only modifies the potentials close to the dissociation threshold limit, i.e., near the Rb($n = 25$) limit. In the lowest wells, where the Rydberg molecules form, the two sets of potentials are slightly shifted with respect to each other while being otherwise almost identical, indicating that including the f -wave quantum defect has almost no influence on the behaviour of the resulting giant molecule, nor on the polyatomic molecular dipole moment.

By including more Rydberg orbitals in our basis set, we can explore the range of validity of the degenerate perturbation theory approach. For smaller dipole moments, $d_0 \lesssim 0.4$ a.u., relatively few basis states are required to achieve convergence. In fact, the converged potentials are only slightly different from those shown in figure 1. As the dipole moment increases, more and more Rydberg orbitals are required. This is due to the localizing effects of the dipole-electron potential. For a nearly critical dipole moment, $d_0 \approx 0.63$ a.u., the electron is almost entirely localized at the location of the dipole. To accurately describe this (small angle) local-

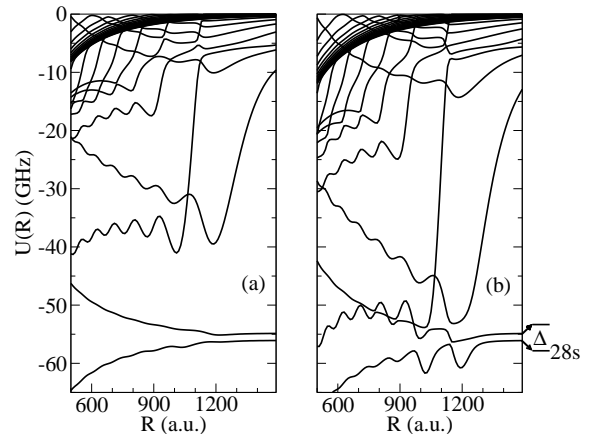


FIG. 2: (a) The BO potentials for the Rydberg-polar molecule system are shown, calculated including lower angular momentum states using a polar molecule Λ -doublet parity splitting of $\Delta = 1.85 \times 10^{-7}$ a.u. and a dipole moment of $d_0 = 0.40$ a.u. (subcritical dipole). (b) The same as (a) with a dipole moment of $d_0 = 0.57$ a.u. (the permanent dipole moment of CD). The zero in energy is the Rb($n = 25$) threshold. The 28s level and zero field molecular splitting have also been labelled.

ization requires an inordinately large number of Rydberg orbitals. Furthermore, for larger values of d_0 , the electron wave function penetrates into the short-range region of the perturber molecule and probes the detailed structure of the molecule. We therefore restrict here to sub-critical dipole moments, $d_0 \leq 0.6$ a.u. Because the Rydberg spacing scales as n^{-3} , larger sets of orbitals are required to converge the potentials attached to higher Rydberg thresholds. The calculations reported here are for Rb($n = 25$) manifold of states, though the qualitative behaviours we discuss will persist for higher n . To acquire converged potentials for $n = 25$ at the largest dipole moments considered here, $d_0 = 0.60$ a.u., our basis includes all electron angular momenta for $n = 19, 20, \dots, 30, 31$ as well as the $32(s, p, d)$, $33(s, p)$ and $34s$ Rydberg orbits, yielding a total of 331 electron basis states.

Figure 2 shows the converged potentials attached to the $n = 25$ Rydberg level. As in figure 1, the polar molecule in figure 2(a) has a dipole moment $d_0 = 0.40$ a.u. and a zero field splitting $\Delta = 1.85 \times 10^{-7}$ a.u. (Δ has been chosen to be the Λ -doublet splitting of CD). Comparing the two figures shows that the molecular potentials are unaffected by the presence of the non-binding s -wave states for cases when the molecular dipole is less than ~ 0.4 a.u. The two curves converging to the Rb(28s) threshold correspond to the two opposite parity states of the polar molecule and are correspondingly split by the zero field splitting Δ .

For larger dipole moments, it is essential to include the lower angular momentum states in our treatment. While for an unperturbed Rydberg atom, the latter are isolated from the degenerate $l > 2$ manifold, increasing

the dipole moment has the interesting effect of forcing the potential wells of the $n = 25$ to cross through the $28s$ potentials. This is possible because the Rb(ns) quantum defect ($\mu_s = 3.13$) has a small non-integer fraction, placing the Rb($28s$) close to the $n = 25$ degenerate manifold of states. In figure 2(b), a corresponding example with $d_0 = 0.57$ a.u. = 1.46 D – the permanent dipole moment of CD – is provided. In this case, the interaction between the $n = 25$ molecular states and the Rb($28s$) state is significant. This is generally true of all Rb($n(l > 2)$) degenerate manifolds and $(n + 3)s$ interacting states. As a result and due to strong avoided crossings, potential wells capable of supporting bound vibrational levels appear in the BO curves attached to the Rb($28s$) threshold. Figure 3(a) provides a close-up of the four BO potentials directly involved in the binding of the polyatomic Rydberg molecule. The vibrational wave functions for two such bound states in the outermost wells are also shown.

V. S-WAVE ADMIXTURE

The BO potential curves in figure 1 (also in [15]) include a nearly degenerate superposition of atomic orbitals. As such, they solely contain contributions from high angular momentum states ($l > 2$) and hence are only accessible in experiments which "photoassociate" these molecules, if and when low-lying angular momenta are admixed into the degenerate manifold. The strong interaction of the $(n + 3)s$ Rydberg state with the lowest BO potential curves belonging to the $n(l > 2)$ manifolds in figure 3(b) admixes large amount of s -wave character into the wave functions.

At the potential minimum, the adiabatic channel function is well approximated by

$$\psi(r, \chi) = a(d_0) \psi_d(\vec{r}) |\chi_d\rangle + b(d_0) \psi_s(r) |\chi_s\rangle, \quad (12)$$

where ψ_d and $|\chi_d\rangle$ are the electronic wave function and internal polar molecule state, respectively, that include higher electron angular momentum with $l > 2$. ψ_s and $|\chi_s\rangle$ are the s -wave Rydberg electron wave function and the corresponding molecular state, respectively. The expansion coefficients $a(d_0)$ and $b(d_0)$ depend on the dipole moment of the polar perturber as well as on its position R . Figure 3(b) gives the s -wave electron contribution, $|b(d_0)|^2$, as a function of the intermolecular separation distance for each of the adiabatic channel functions corresponding to the potentials shown in figure 3(a). From figure 3(b) it can be seen that near the minima of the outer wells, the electronic state of the giant molecule has a significant s -wave character, approximately 30 – 40%. This implies the possibility that these molecules could be formed in a simple two photon excitation scheme similar to that used in the experimental realization of homonuclear Rydberg molecules [8]. The $n = 25$ wells shown in figure 3(a) are deep enough to support bound vibrational states, the radial wave functions of the first two

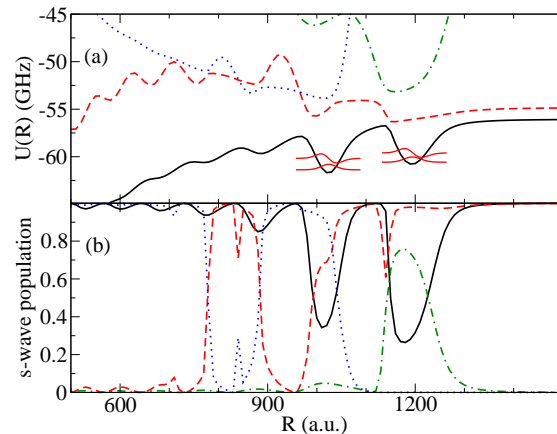


FIG. 3: (a) The four BO potentials, directly involved in molecular binding, are shown for the same parameters as in figure 2(b). Two vibrational wave functions are also shown at their binding energies in each of the outermost wells. (b) The s -wave character of the molecular wave function is shown for each of the four potentials.

such states are shown at their corresponding binding energies in the outer two wells. These molecular levels are well isolated and have readily accessible vibrational frequencies.

The added s -wave character in the electron wave function decreases the charge localization exhibited in the Rydberg molecule slightly. Even with this decrease, these Rydberg molecules exhibit massive dipole moments. Using the scaling behaviour of [15], the Rydberg molecule dipole moment d_{Ryd} can be found,

$$d_{Ryd} \approx 1.3 [a(d_0)]^2 n^2.$$

For the case shown in figure 3(a) this yields $d_{Ryd} \approx 1400D$, a truly large dipole moment. The presence of these enormous dipole moments indicates that the polyatomic Rydberg molecules could be sensitively controlled through the use of small external electric fields. Due to the extreme sensitivity of Rydberg electron to external fields, the behaviour of the BO potentials under the influence of such fields is not immediately obvious and is the subject of ongoing studies.

In figure 4(a-c), we provide snapshots of additional BO potentials responsible for molecular binding, namely, for $d_0 = 0.30, 0.55,$ and 0.60 a.u., respectively. As the dipole moment of the polar perturber increases, the L and R wells are pulled down through the s -wave Rydberg threshold. At $d_0 = 0.30$ a.u., the well structure is not perturbed at all by the s -wave potential. For $d_0 = 0.55$, the potential wells are strongly distorted by the presence of the lower threshold, while for $d_0 = 0.60$ a.u. the outermost well structures have passed through the s -wave threshold and correspondingly have a much smaller s -wave contribution. Figures 4(d-f) show the s -wave electron contribution for each potential. For 0.5

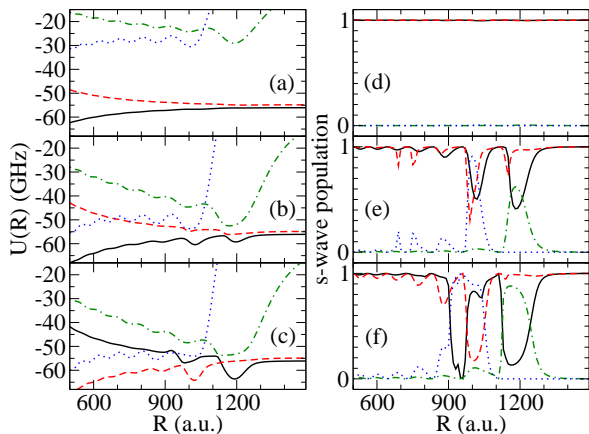


FIG. 4: The variations of the BO potential curves with the strength of the polar molecule dipole moment d_0 . (a) $d_0 = 0.30$ a.u., (b) $d_0 = 0.55$ a.u., and (c) $d_0 = 0.60$ a.u. The respective s -wave contributions to the molecular wave functions are shown in panels (d-f). A Λ -doublet parity splitting of $\Delta = 1.85 \times 10^{-7}$ a.u. is considered.

a.u., $d_0 \lesssim 0.6$ a.u. the s -wave character at the position of the outermost wells varies approximately 10 – 40%, enough to give a fairly large Rabi frequency for the creation of Rydberg molecules in a standard two photon excitation scheme.

VI. CONCLUSIONS AND OUTLOOK

In this paper we have examined the formation of giant, polyatomic Rydberg molecules consisting of a Λ -doublet polar molecule and a Rydberg atom. We provided a more complete description of the polar molecule model initially used to predict these nearly macroscopic molecules [15]. By using a two-state model that is sensitive to external fields, a Rydberg electron is coupled to the internal state of the polar molecule. The resulting electron-molecule

interaction creates a series of BO potentials with an oscillating series of wells that reflect the Rydberg oscillations in the electron wave function. By extending the work in [15] to beyond the degenerate perturbation theory, we have shown that the small, but finite f -wave quantum defect changes little the behaviour of the resulting giant molecules.

By including lower electron-angular momentum states, a new set of potentials attached to the $(n+3)s$ Rydberg level appear. These added potentials have no significant influence on electronic state of the Rydberg molecule for smaller subcritical dipole moments, $d_0 \lesssim 0.4$ a.u. For nearly critical dipole moments, $d_0 \approx 0.6$ a.u., a series of avoided and level crossings is formed between the potentials formed from the degenerate $n(l > 2)$ manifold and the $(n+3)s$ -wave potentials. These avoided crossings lend significant s -wave character to the Rydberg electron state opening the possibility of creating the giant polyatomic Rydberg molecules using standard two-photon Rydberg excitation schemes. The series of avoided and level crossings create a complex structure of couplings between the various BO potentials. Extensions of this work beyond a simple two-state polar molecule to incorporate rigid rotor-type polar molecules, such as KRb, poses a significant challenge. The added angular behaviour of the polar molecule will create a set of two-dimensional potential surfaces which couple the rotational behaviour of the polar molecule to the vibrational state of the giant Rydberg molecule. Creating and examining this intricate energy landscape will be the subject of future work.

VII. ACKNOWLEDGEMENTS

The authors would like to thank T. V. Tscherbul for help in calculating the Λ -doublet molecule parameters used in this work. MM acknowledges financial support from the German Academic Exchange Service (DAAD). STR and HRS acknowledge financial support from the NSF through ITAMP at Harvard University and the Smithsonian Astrophysical Observatory.

-
- [1] M. SAFFMAN, T. G. WALKER, and K. MØLMER, *Rev. Mod. Phys.* **82**, 2313 (2010).
 - [2] T. F. GALLAGHER, *Rydberg Atoms*, Cambridge University Press, Cambridge, U.K., 1994.
 - [3] W. R. ANDERSON, J. R. VEALE, and T. F. GALLAGHER, *Phys. Rev. Lett.* **80**, 249 (1998).
 - [4] E. URBAN, T. A. JOHNSON, T. HENAGE, L. ISENHOWER, D. D. YAVUZ, T. G. WALKER, and M. SAFFMAN, *Nat. Phys.* **5**, 110 (2009).
 - [5] A. GAËTAN, Y. MIROSHNYCHENKO, T. WILK, A. CHOTIA, M. VITEAU, D. COMPARAT, P. PILLET, A. BROWAEYS, and P. GRANGIER, *Nat. Phys.* **5**, 115 (2009).
 - [6] T. WILK, A. GAËTAN, C. EVELLIN, J. WOLTERS, Y. MIROSHNYCHENKO, P. GRANGIER, and A. BROWAEYS, *Phys. Rev. Lett.* **104**, 010502 (2010).
 - [7] L. ISENHOWER, E. URBAN, X. L. ZHANG, A. T. GILL, T. HENAGE, T. A. JOHNSON, T. G. WALKER, and M. SAFFMAN, *Phys. Rev. Lett.* **104**, 010503 (2010).
 - [8] V. BENDKOWSKY, B. BUTSCHER, J. NIPPER, J. P. SHAFER, R. LOW, and T. PFAU, *Nature* **458**, 1005 (2009).
 - [9] T. KILLIAN, T. PATTARD, T. POHL, and J. ROST, *Phys. Rep.* **449**, 77 (2007).
 - [10] T. POHL, H. SADEGHPOUR, and P. SCHMELCHER, *Phys. Rep.* **484**, 181 (2009).
 - [11] T. POHL, E. DEMLER, and M. D. LUKIN, *Phys. Rev. Lett.* **104**, 043002 (2010).
 - [12] B. OLMOS, R. GONZÁLEZ-FÉREZ, and I. LESANOVSKY,

- Phys. Rev. Lett.* **103**, 185302 (2009).
- [13] N. TEZAK, M. MAYLE, and P. SCHMELCHER, *arXiv:1012.3810v1 [physics.atom-ph]*.
- [14] L. D. CARR, D. DEMILLE, R. V. KREMS, and J. YE, *New Journal of Physics* **11**, 055049 (2009).
- [15] S. T. RITTENHOUSE and H. R. SADEGHPOUR, *Phys. Rev. Lett.* **104**, 243002 (2010).
- [16] C. H. GREENE, A. S. DICKINSON, and H. R. SADEGHPOUR, *Phys. Rev. Lett.* **85**, 2458 (2000).
- [17] V. BENDKOWSKY, B. BUTSCHER, J. NIPPER, J. B. BALEWSKI, J. P. SHAFFER, R. LÖW, T. PFAU, W. LI, J. STANOJEVIC, T. POHL, and J. M. ROST, *Phys. Rev. Lett.* **105**, 163201 (2010).
- [18] B. BUTSCHER, J. NIPPER, J. B. BALEWSKI, L. KUKOTA, V. BENDKOWSKY, R. LOW, and T. PFAU, *Nat. Phys.* **6**, 970 (2010).
- [19] J. E. TURNER, *Am. J. Phys.* **45**, 758 (1977).
- [20] M. MARINESCU, H. R. SADEGHPOUR, and A. DALGARNO, *Phys. Rev. A* **49**, 982 (1994).
- [21] J. D. JACKSON, *Classical Electrodynamics*, Wiley, New York, USA, third edition, 1999.
- [22] E. HAMILTON, C. GREENE, and H. SADEGHPOUR, *J. Phys. B* **35**, L199 (2002).
- [23] M. CHIBISOV, A. KHUSKIVADZE, and I. FABRIKANT, *J. Phys. B* **35**, L193 (2002).